Colloid Polym Sci (2005) 283: 636–645
DOI 10.1007/s00396-004-1194-0

ORIGINAL CONTRIBUTION

Huawei Wu
Seigou Kawaguchi
Koichi Ito

^{1}H NMR studies on intermolecular association of amphiphilic cationic polyelectrolyte micelles induced by hydrophobic counteranions in water

Received: 19 January 2004
Accepted: 8 June 2004

H. Wu · K. Ito
Department of Materials Science,
Toyohashi University of Technology,
Tempaku-cho, 441-8580 Toyohashi, Japan

S. Kawaguchi (✉)
Department of Polymer Science
and Engineering, Yamagata University,
4-3-16 Jonan, 992-8510 Yonezawa, Japan
E-mail: skawagu@yz.yamagata-u.ac.jp
Tel.: +81-238-263182
Fax: +81-238-263182

Abstract Interactions of a series of amphiphilic cationic polyelectrolytes with various kinds of organic counteranions have been investigated in water by one- and two-dimensional ^{1}H NMR spectroscopy at 20 °C. The cationic polyelectrolytes were prepared by micellar homopolymerization of tail-type cationic surface-active monomers with a cationic charge with ω-end, (ST–C$_m$–AB, $m = 5$, 7, and 9, where ST is a styrenic group, C$_m$, an alkylene chain at the 4-position of styrene, and AB, alkyltrimethylammonium bromide). Aliphatic monosodium salt of maleic acid (MAS) and its stereoisomer, fumaric acid (FAS), sodium benzoate (NaB), potassium hydrogen phthalate (PHK), and sodium salicylate (NaSal) were added to a salt-free aqueous solution of the polyelectrolytes and ^{1}H NMR measurements were carried out. Amphiphilic P(ST–C$_m$–AB) polyelectrolytes act as efficient hosts to strongly capture the hydrophobic counteranions B$^-$, PH$^-$, and Sal$^-$, but not MA$^-$ and FA$^-$. The ^{1}H NMR signals of these hydrophobic counteranions remarkably shift upfield and broaden in water in the presence of the amphiphilic polyelectrolytes. The nuclear Overhauser effect (NOE) signals between the cationic group of the polymer and aromatic benzoate counteranion protons are clearly observed to imply cation–π interaction. The capturing of hydrophobic counterions by the polyelectrolytes is likely due to electrostatic, hydrophobic, and cation–π interactions between them. The reduced viscosity, η_{sp}/C_p, for the solution at [PHK]/[P(ST–C$_7$–AB)] = 1.0 steeply increases with increasing polymer concentration (C_p) above ca. 0.9 g/dL to show pronounced viscoelasticity.

Keywords Polymerizable surfactants · Polymeric micelle · Solubilization · Cation–π interaction · Host–guest interaction · Cationic polyelectrolyte

Introduction

Surfactant molecules in aqueous solution self-assemble into micellar aggregates. A variety of aggregate structures can form such as spherical or rodlike micelles, vesicles, or lamellar phases [1]. Most applications of the surfactants make use of this ability to self-assemble and their dynamic response to changing solution conditions. Polymeric and oligomeric surfactants are superior to low molecular weight surfactants in forming large aggregates and in stabilizing the shapes against changes in circumstances [2, 3, 4, 5]. Surfactants with a polymerizable functional group are often used for stabilization of the organized structures such as vesicles [6], spherical micelles [7], lamellae [8] or hexagonal arrays of cylinders [9], and rodlike micelles [10]. In fact, Kline demonstrated that a rodlike micelle from cetyltrimethylammonium 4-vinylbenzoate was stabilized by micellar radical polymerization of the vinylic group of the counteranion [10]. The resulting polymer micelle, as observed by small-angle neutron scattering, is likely to retain its original rodlike architecture, which shows an enhanced thermal stability and no longer dissociates upon dilution. Shikata and coworkers studied the viscoelastic behavior of hybrid threadlike micelle solutions formed by cetyltrimethylammonium bromide (CTAB) and sodium salicylate (NaSal) [11], CTAB, sodium *p*-toluenesulfonate, and sodium poly(*p*-vinylbenzoate) [12, 13].

Recently, we reported that homo- and copolymerization of a series of novel tail-type cationic surface-active monomers with a cationic charge with *ω*-end, (ST–C_m–AB, $m = 5$, 7, and 9, where ST is a styrenic group, C_m, an alkylene chain at the 4-position of styrene, and AB, alkyltrimethylammonium bromide) proceeds very rapidly in water to afford the corresponding cationic polyelectrolytes with high molecular weights [14]. Their fundamental physicochemical properties such as critical micelle concentration (cmc) and weight-averaged aggregation number of the micelle ($N_{\mathrm{w(agg)}}$) have been characterized in water at 25 °C and related to the polymerization behavior. The tail-type cationic polyelectrolytes with long alkylene chain, P(ST–C_m–AB), were interestingly soluble in water and appear to assume unimolecular, micelle-like, and compact conformation. Furthermore, addition of hydrophobic counteranions such as potassium hydrogen phthalate (PHK) and NaSal induced intermolecular aggregation among the polyelectrolyte micelles to increase solution viscosity, and produce the gel and precipitation at high polyelectrolyte concentration [14].

Here, we report one- and two-dimensional ^{1}H NMR studies on interactions of small organic molecules with the polymeric micelles, especially in regard to the effects of structure of the polyelectrolytes and organic counteranions on the selectivity and specificity, as shown in Scheme 1.

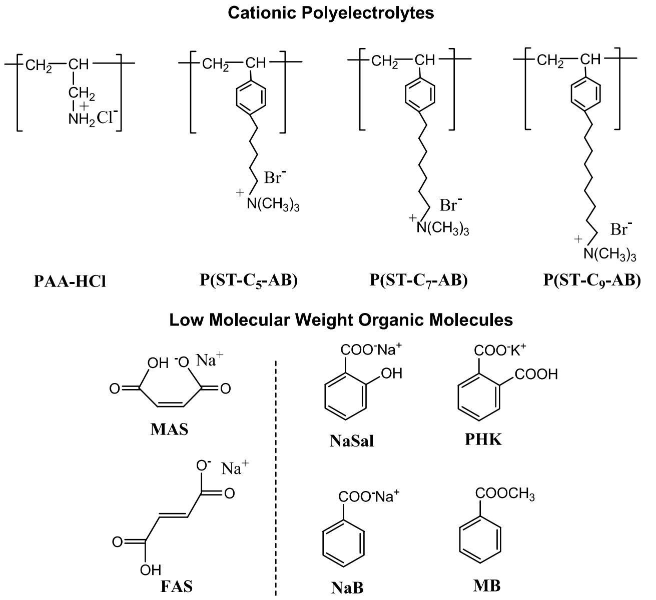

Scheme 1 Cationic polyelectrolytes and low molecular weight organic molecules used in this study

Experimental

Materials

Poly(allylammonium chloride) (PAA-HCl$^-$ 10L, $M_w = 1.5\times10^5$) was purchased from Nitto Boseki Co.

Fig. 1 ^{1}H NMR spectra of ST–C_7–AB micelles **a** before and **b** after loading PHK in D_2O at 20 °C: [ST–C_7–AB] = 1.0×10^{-2} M; [PHK]/[ST–C_7–AB] = 3.0

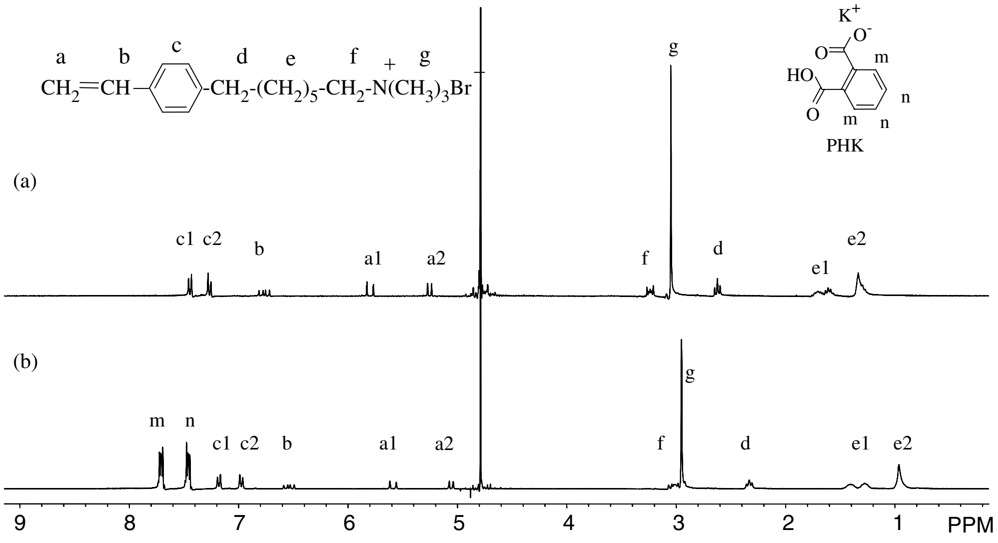

Table 1 Chemical shifts (in ppm) of ST–C_7–AB (0.01 M) and PHK at different [PHK]/[ST–C_7–AB]

[PHK]/[ST–C_7–AB]	c1	c2	b	a1	a2	f	g	d	e1	e2
0	7.447	7.277	6.786	5.811	5.266	3.246	3.059	2.630	1.655	1.343
0.5	7.387	7.209	6.717	5.761	5.216	3.169	3.035	2.561	1.587	1.256
0.8	7.348	7.160	6.686	5.721	5.185	3.165	3.022	2.512	1.529	1.208
1.0	7.323	7.126	6.652	5.696	5.160	3.131	3.006	2.470	1.495	1.156
2.0	7.232	7.026	6.579	5.623	5.095	3.049	2.968	2.378	1.386	1.029
3.0	7.185	6.979	6.541	5.585	5.049	3.020	2.949	2.332	1.331	0.955

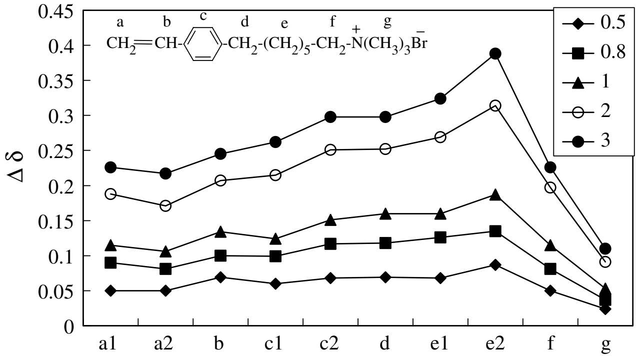

Fig. 2 Change in proton chemical shifts (Δδ in ppm) for ST–C_7–AB with [PHK] at 20 °C: [ST–C_7–AB] = 1.0×10^{-2} M; [PHK]/[ST–C_7–AB] = 0.5 (◆), 0.8 (■), 1.0 (▲), 2.0 (○), and 3.0 (●)

Ltd. All samples of the cationic surface-active monomers and the corresponding cationic homopolymers were synthesized as described in the previous report [14]. The homopolymers were purified by dialysis against deionized water for 1 week and recovered by freeze-drying. Water was purified with a Millipore Milli-Q purification system and used within a few hours. Organic salts were of the highest grade available and used without further purification.

Measurements

One-dimensional ^{1}H NMR spectra were recorded on a Varian Mercury 300 spectrometer. The condition was 16 times accumulation and 30 s pulse delay time. Two-dimensional ^{1}H–^{1}H NOESY was run with a Varian INOVA 500 spectrometer. The trace of H_2O (δ = 4.79 ppm) in D_2O solvent was used as an internal reference for the proton spectrum. All NMR measurements were carried out at 20 °C.

Viscometry measurement was carried out using a four-bulb low-shear Ubbelohde-type capillary viscometer at 25 °C [15].

Results and discussion

NMR spectroscopy is a most powerful technique to allow one to investigate the microscopic behavior and dynamics of molecules in solution. It can focus on a chemical circumstance around individual functional groups or atoms as well as their motional information by use of chemical shifts and relaxation behavior. NMR methods have been regularly employed in the study of micellar solutions. Although aromatic molecules like benzene and indole have a relatively high solubility in water, in fact it was observed by NMR spectroscopy that they are solubilized in the interfacial region of amphiphilic aggregates [16, 17]. The most frequently encountered technique to probe the binding location of aromatic compounds in micelles is to use changes in the chemical shifts in the ^{1}H NMR spectrum of the surfactant induced by the ring current of the aromatic moiety of the solubilizate [18, 19, 20, 21, 22].

We first report ^{1}H NMR studies on the interactions between ST–C_7–AB micelle with hydrophobic counteranion PHK, followed by the interactions between the cationic polyelectrolytes and various counteranions. Finally we discuss intermolecular association of polyelectrolytes upon the addition of PHK molecules.

Interactions between ST–C_7–AB micelle and PHK

Figure 1 shows the ^{1}H NMR spectra of ST–C_7–S–AB micelles of concentration above the critical micelle concentration (cmc = 1.1 mmol/L) [14] before and after loading PHK in D_2O at 20 °C. One clearly finds that all proton signals of ST–C_7–AB are significantly shifted upfield upon addition of PHK, implying that ST–C_7–AB micelles interact with PH^- molecules. The broadening of the proton signals of the micelle and PH^-, however, is not observed, presumably due to rapid exchange in PH^- molecules between the bulk and micelle phases. Another reason may be due to the fact that the interactions between the micelle and PH^- are too weak to restrict their motion. To investigate the behavior of PH^- molecules in the ST–C_7–AB micelles in detail, the chemical shift difference (in ppm) of each proton of ST–C_7–S–AB micelles before and after loading PHK is investigated as a function of PHK concentration and shown in Table 1 and Fig. 2.

Three interesting observations are that the ring current-induced upfield shifts by PH^- take place for all protons of the micelle, that the extent of the shift

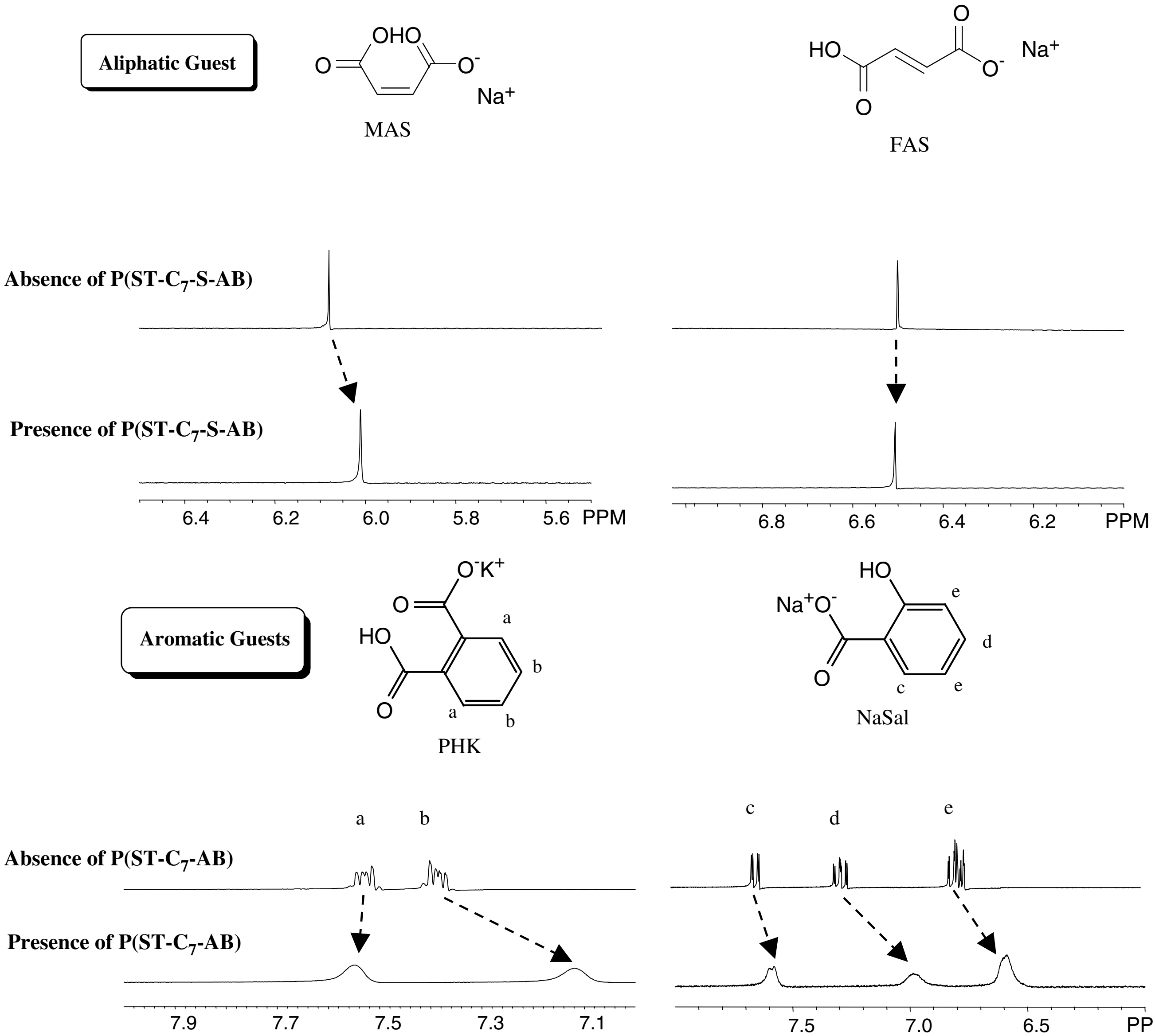

Fig. 3 ^{1}H NMR signal change of aliphatic and aromatic guest molecules in the presence of P(ST–C$_7$–AB): [P(ST–C$_7$–AB)] = 1.0×10^{-2} N and [guest]/[P(ST–C$_7$–AB)] = 1.0

increases with increasing PHK concentration, and that the shift is remarkable in the proton signals of the alkylene chain (peak e) in the vicinity of ω-charge.

The dynamics of incorporation into micelles are similar to those observed for entry and exit of individual surfactant molecules. Their uptake into micelles is close to diffusion controlled, whereas the residence time in micelles depends on the structure of the micelle and solubilizate, and is typically in the order of 10^{-4} to 10^{-6} s [23, 24]. Hence, these processes are fast on the NMR timescale. The time-averaged location of aromatic hydrocarbons in or at the micelle has been intensively debated. Investigations have focused on the distribution of benzene in aqueous solutions of CTAB and sodium dodecyl sulfate (SDS). Some authors have claimed that the benzene molecule mainly resides in the interior of these micelles [25, 26, 27]. Others have reported that binding occurs at the interface between micelle and water [28, 29] or in both regions [30]. Shikata et al. also reported that the CTAB micelle forms complexes with Sal$^-$ counterions through electrostatic interactions in aqueous solution, and Sal$^-$ molecules are located in the head group of the CTAB micelle [11]. From the present experimental observations, one can conclude that PH$^-$ ions can move with high mobility in the ST–C$_7$–AB micelles but the time-averaged location of PH$^-$ ions in the micelles is the alkylene chain near the cationic charge.

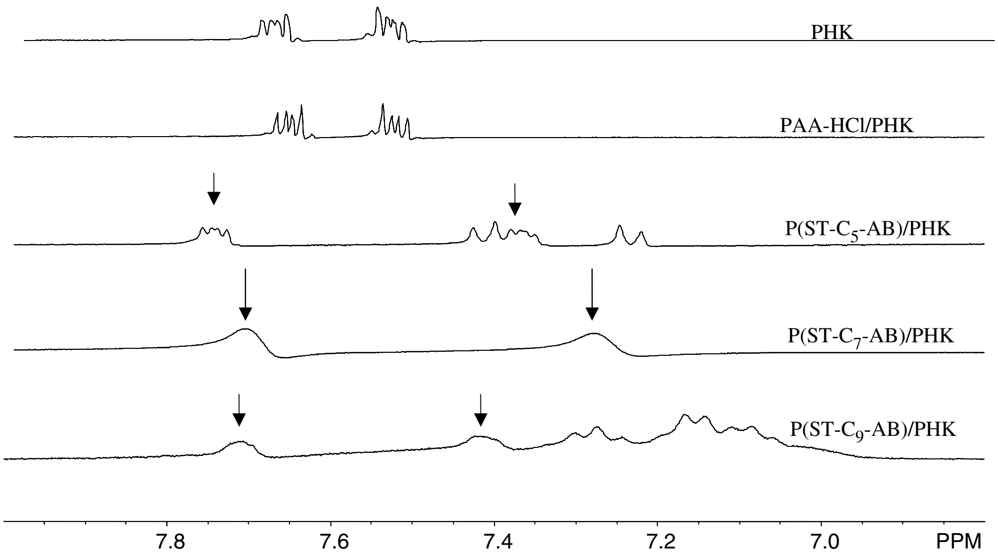

Fig. 4 ^{1}H NMR signals of aromatic protons of PHK in the absence and presence of different cationic polymers: [PHK] = 1.0×10^{-3} M and [polyelectrolytes] = 1.0×10^{-3} N

Interactions of P(ST–C_7–AB) with hydrophobic counterions

In our previous studies, we found that the addition of hydrophobic counteranions with a weak acid group such as PHK and NaSal to a salt-free aqueous solution of P(ST–C_7–AB) promotes intermolecular aggregation to increase solution viscosity at high polyelectrolyte concentrations [14]. ^{1}H NMR studies were carried out to obtain information about the interactions between P(ST–C_7–AB) and various kinds of organic counteranions.

Figure 3 shows the ^{1}H NMR spectra of aliphatic and aromatic counteranions before and after loading P(ST–C_7–AB). It may be worth noting that in the

Fig. 5 Change in ^{1}H NMR spectra of NaB with different [NaB]/[P(ST–C_7–AB)]; [P(ST–C_7–AB)] = 1.0×10^{-2} N

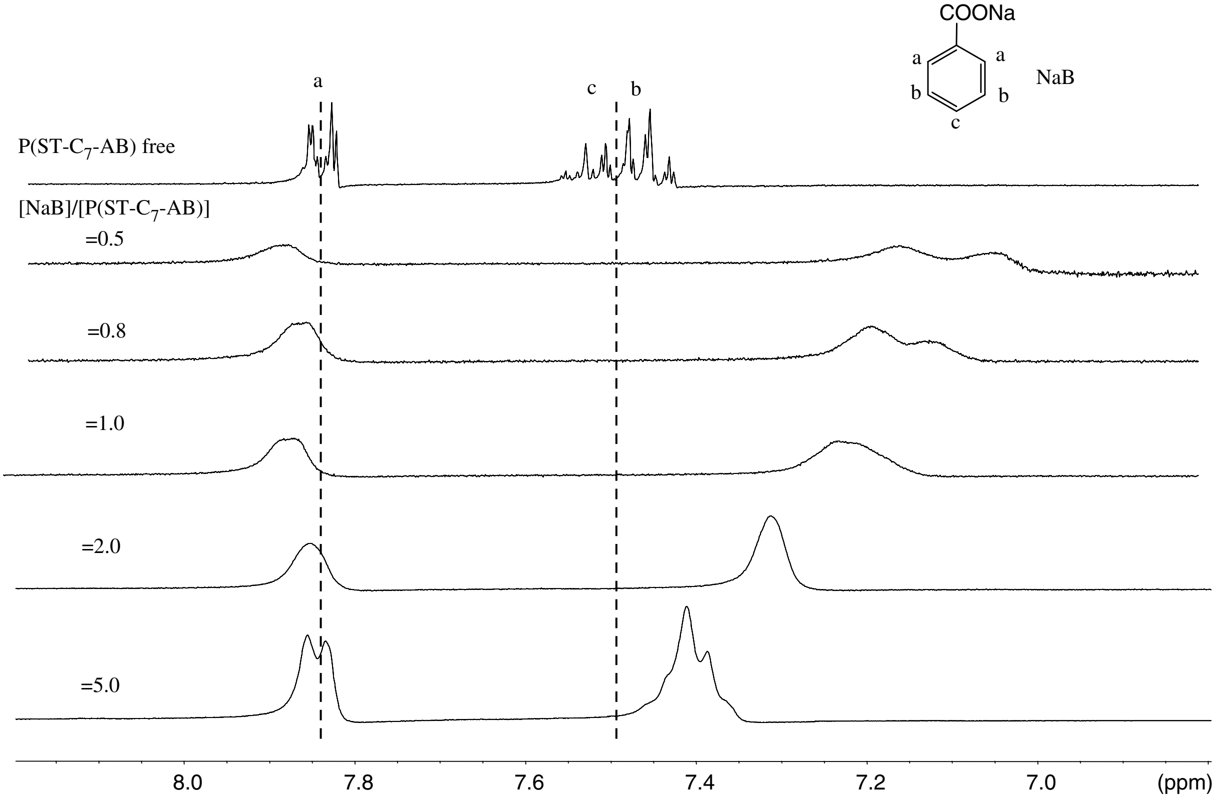

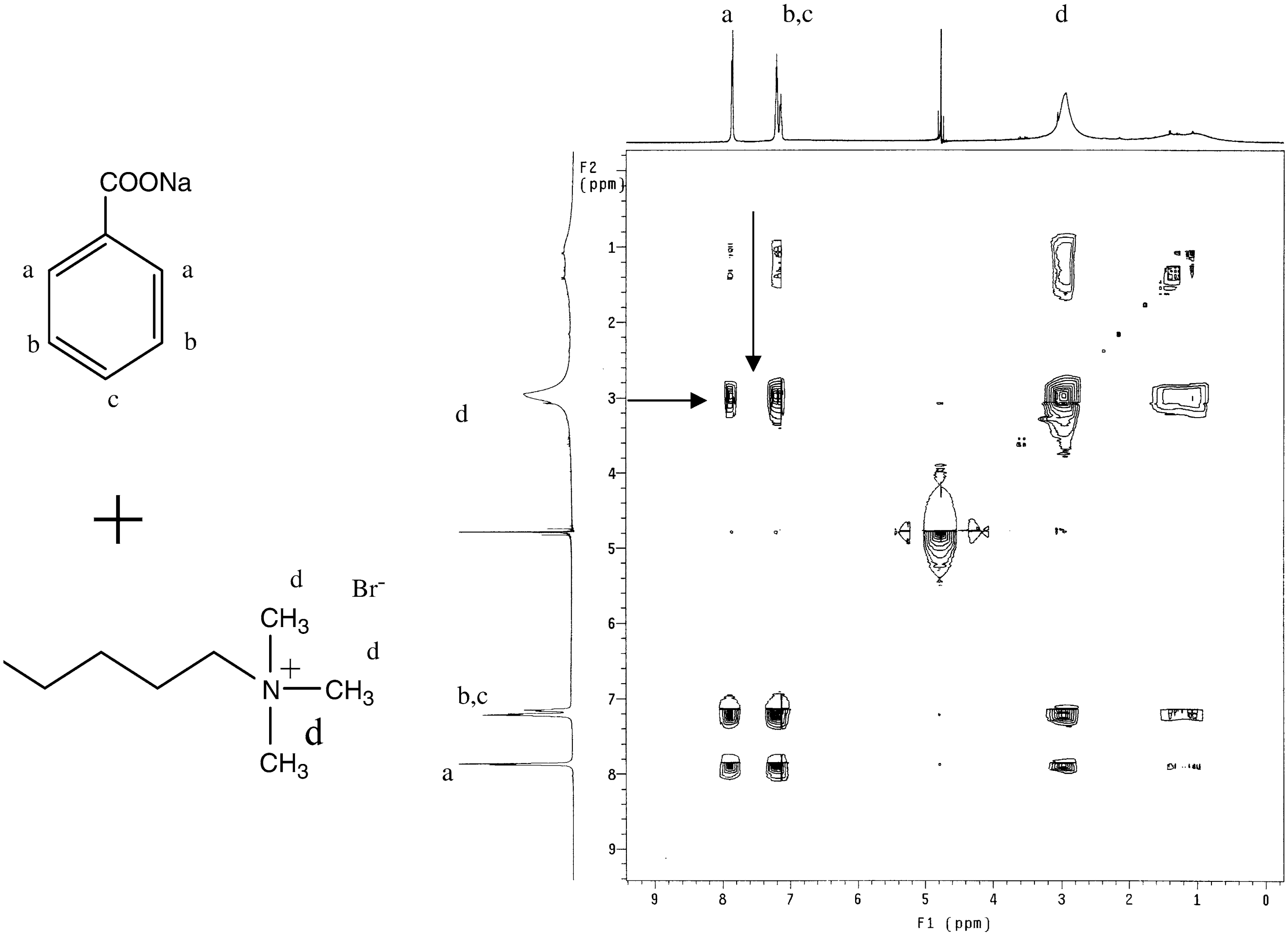

Fig. 6 Two-dimensional 500 MHz ^1H–^1H NOESY of [NaB]/[P(ST–C_7–AB)] = 1.0; [P(ST–C_7–AB)] = 5.0×10^{-2} N

cases of PHK and NaSal, the ^1H NMR peaks of the aromatic protons are shifted and broadened by the presence of the P(ST–C_7–AB). This may imply the existence of strong interactions between hydrophobic counteranions, PH$^-$ or Sal$^-$, and the P(ST–C_7–AB) micelle.

On the other hand, in the case of the aliphatic anions maleic acid monosodium salt (MAS) and its stereoisomer and fumaric acid monosodium salt (FAS), such broadening is not observed which implies lack of the strong interaction. A particularly interesting experimental observation to be noted in the latter case is the difference in the behavior between MA$^-$ and FA$^-$. One sees that the ^1H NMR peak of MA$^-$ slightly shifts to upfield in the presence of the P(ST–C_7–AB), indicating the presence of weak interactions between them. Since the water solubility of these salts is almost the same [31], any structural difference between these salts, such as the intramolecular hydrogen bond in MA$^-$, is likely responsible for the molecular recognition.

According to the “counterion condensation theory” of polyelectrolyte solutions, the counterions Br$^-$, PH$^-$, Sal$^-$, MA$^-$, and FA$^-$ are thought to be equally condensed on a polyelectrolyte chain, leading to the decrease of their activity [32]. The fraction of condensed counterions is proportional to the charge density of the polyelectrolyte. The difference in the selectivity between hydrophobic and hydrophilic counteranions is a very interesting subject to be clarified.

The trend in chemical shift of the aromatic protons also provides additional information on the location of PHK or NaSal in the polymer micelles. When PHK is introduced into the polymeric micelles the NMR signals of protons (b) shift toward a lower chemical shift, compared to that of protons (a) which remain unchanged. This suggests that protons (b) are located in a more nonpolar environment among the polymer micelles. Thus, the aromatic ring of a PH$^-$ ion may locate in the vicinity of the ammonium head groups on the surface of the polymer micelle and its polar functional groups are directed to the water phase. A similar observation is seen in the case of Sal$^-$ as a counteranion.

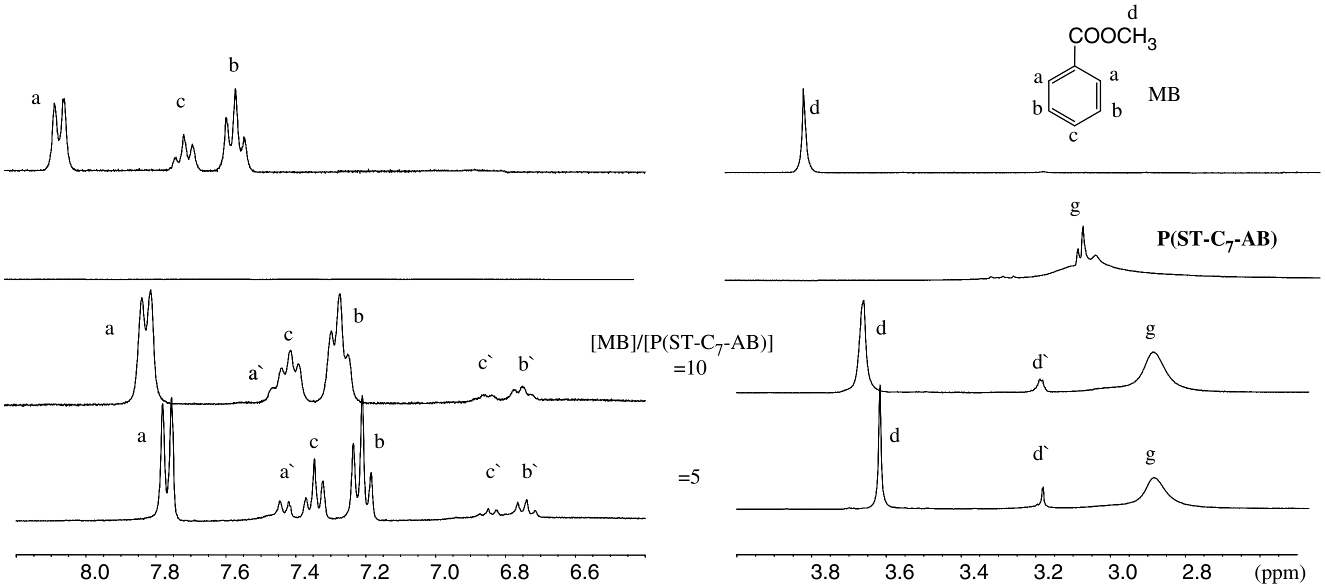

Fig. 7 ^{1}H NMR spectra of MB molecules in the absence and presence of P(ST–C_7–AB): [MB] = 1.0×10^{-1} M

Interactions between PHK and different cationic polyelectrolytes

To estimate the influences of molecular structure of the cationic polyelectrolytes on the interactions with PH^- anions, ^{1}H NMR measurements were carried out for the PHK solution containing the polyelectrolytes listed in Scheme 1. Figure 4 shows the ^{1}H NMR spectra of PH^- molecules in the absence and presence of different cationic polyelectrolytes. When poly(allylammonium chloride) ($PAAH^+Cl^-$) as a general hydrophilic, cationic, linear, flexible polyelectrolyte chain is added to PHK solution, no broadening and chemical shift of PH^- aromatic signals are observed, implying the lack of strong interactions between them. On the other hand, the ^{1}H NMR signals of PH^- are slightly broadened by the presence of the P(ST–C_5–AB) chain but noticeably more by P(ST–C_7–AB) and P(ST–C_9–AB). This trend demonstrates that for efficient interactions, the cationic polyelectrolyte chain needs to have at least a hydrophobic part to probably form a micelle structure. The organized structure with hydrophobic and hydrophilic regions, as well as the compact conformation with high charge density, may facilitate the interactions with hydrophobic counteranions.

Cation–π interaction between NaB and P(ST–C_7–AB)

Figure 5 shows typical NMR signal changes of phenyl protons of NaB as a function of mole ratio of [NaB]/[P(ST–C_7–AB)], where [P(ST–C_7–AB)] = 1.0×10^{-2} N and [NaB] varies from 5×10^{-3} to 0.05 M. It may be worth noting that aromatic counteranions without an acidic group near charged B^- molecules are also strongly attracted to the amphiphilic micelle, which supports the view that electrostatic and hydrophobic interactions play an important role in this behavior. One finds remarkable upfield shifts of the (b) and (c) protons of the B^- ion. The peak positions, however, go back to those of free B^- with increasing [NaB]/[P(ST–C_7–AB)]. This is simply due to the increase of concentration of free counteranion with increase of [NaB]/[P(ST–C_7–AB)].

The 500 MHz ^{1}H–^{1}H NOESY results are presented in Fig. 6 for the solution containing [P(ST–C_7–AB)] = 0.05 N and [NaB] = 0.05 M. One sees clear NOE signals (indicated by the arrows), ascribed to a nuclear Overhauser effect between methyl protons (d) of the quaternary ammonium group of the P(ST–C_7–AB) and aromatic protons (a and b) of the benzoate anion. This experimental observation shows that the benzoate anion is exclusively localized in the vicinity of cationic charge of the polymer chain, likely due to "cation–π" interaction [12, 13].

Solubilization of MB into P(ST–C_7–AB) micelles

Figure 7 shows the ^{1}H NMR spectra of the methyl benzoate (MB) molecule without charge before and after loading P(ST–C_7–AB) in D_2O at [MB] = 0.1 M and [P(ST–C_7–AB)] = 0.01 and 0.02 N. When P(ST–C_7–AB) is added into the MB solution, all proton resonance peaks of MB are shifted upfield. The resonance of peak g (ammonium group) of P(ST–C_7–AB) is also shifted. The broadening of the peak signals of MB, however, is not observed, which implies rapid exchange of MB between micelle and water. In other

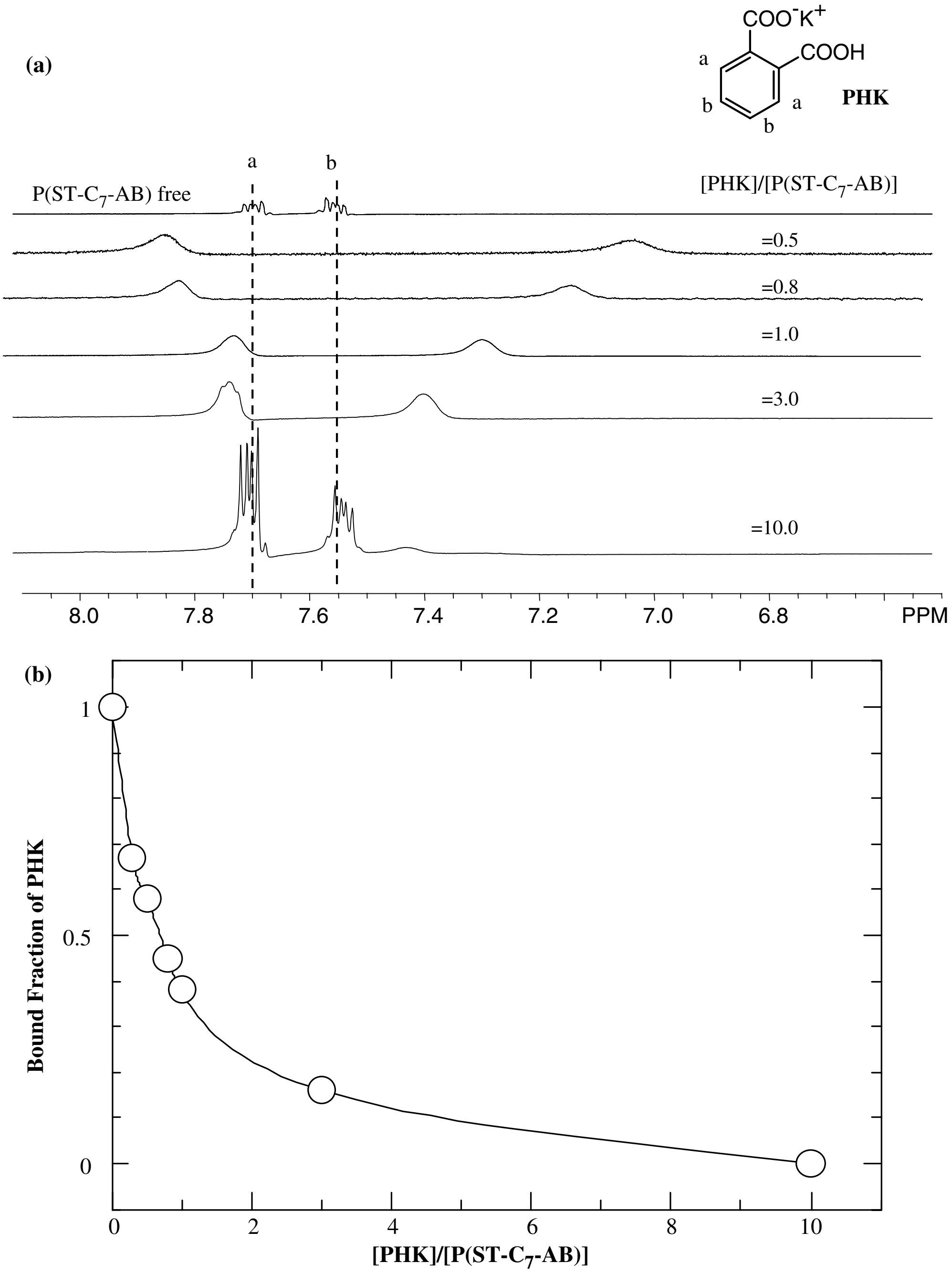

Fig. 8 **a** Change in ^{1}H NMR spectra of PHK with different [PHK]/[P(ST–C_7–AB)]; [P(ST–C_7–AB)] = 1.0×10^{-2} N. **b** Plots of bound fraction of PHK molecules vs [PHK]/[P(ST–C_7–AB)]

words, MB molecules are simply solubilized into the hydrophobic domain of the micelle with sufficient mobility. It is worth noting that the peak signals of MB are further separated into two kinds of peaks, denoted by a, b, c, and d and a′, b′, c′, and d ′ in Fig. 7. The signals a, b, c, and d shift toward the higher magnetic field as [P(ST–C_7–AB)] increases, but a′, b′, c′, and d′ keep their position. The latter peaks may be due to those solubilized deep inside the micelle.

Determination of fraction of PHK molecules bound to P(ST–C_7–AB)

Figure 8a shows NMR signal changes of phenyl protons of PHK as a function of mole ratio of [PHK]/[P(ST–C_7–AB)], where [P(ST–C_7–AB)] = 1.0×10^{-2} N and [PHK] varies from 5×10^{-3} to 0.1 M. ^{1}H NMR spectroscopy is a useful technique for the investigation of the rapid reversible complexation [33, 34, 35, 36, 37]. We paid attention to the NMR signal of the ring protons of PHK

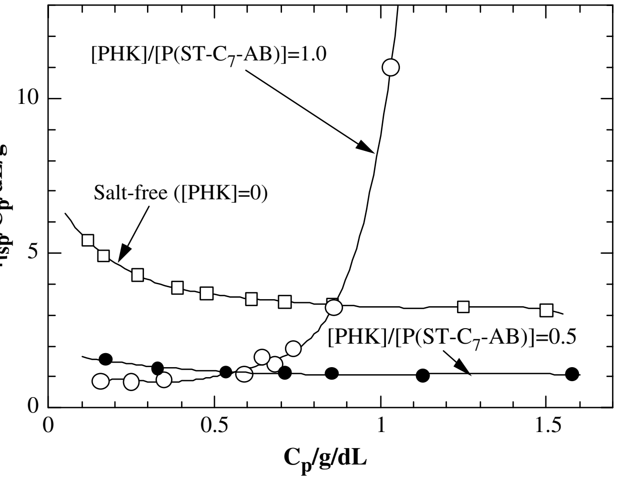

Fig. 9 Huggins plots of η_{sp}/C_p vs C_p at 25 °C; salt-free solution (□), [PHK]/[P(ST–C$_7$–AB)] = 0.5 (●), [PHK]/[P(ST–C$_7$–AB)] = 1.0 (○)

shown in Fig. 8a. The resonance peak of the proton changes the position due to the chemical shift when the PH$^-$ ions of PHK are transferred from the bulk aqueous phase into the micelles. If the exchange rate of PH$^-$ ions between the two states is fast enough to cause a single time-averaged spectrum to appear, the position of the chemical shift v in the frequency is expressed as

$$v = \left(1 - f_{\mathrm{aq}}\right) v_{\mathrm{mic}} + f_{\mathrm{aq}} v_{\mathrm{aq}} \tag{1}$$

where f_{aq} is the fraction of the protons in the aqueous phase and v_{mic} and v_{aq} are the chemical shifts in the micelle and bulk aqueous phase, respectively.

If one replaces the chemical shift v expressed in the frequency unit by that given in the ppm unit (δ), f_{aq} may be rewritten as [11]

$$f_{\mathrm{aq}} = \frac{\delta - \delta_{\mathrm{mic}}}{\delta_{\mathrm{aq}} - \delta_{\mathrm{mic}}} \tag{2}$$

We determine δ_{mic} to be 6.64 ppm for PHK by extrapolating to [PHK]/[P(ST–C$_7$–AB)] = 0. Using the values of δ_{mic} and Eq. 2, the fraction of PHK bound to the polyelectrolyte chain, (1–f_{aq}), is estimated and plotted against [PHK]/[P(ST–C$_7$–AB)], as shown in Fig. 8b. One sees that the fraction of PHK molecules strongly bound to P(ST–C$_7$–AB) steeply decreases with [PHK]/[P(ST–C$_7$–AB)] in [PHK]/[P(ST–C$_7$–AB)] < 1.0, but gradually decreases above it. At [PHK]/[P(ST–C$_7$–AB)] = 1.0, about 38% of the total PHK molecules are strongly bound to the polyelectrolyte chain, in dynamic equilibrium with 62% free PHK molecules in the water phase. ^{1}H NMR just observes the resonances of the time-averaged species between them.

PHK-induced intermolecular association

Figure 9 shows Huggins plots for the dilute aqueous solution of P(ST–C$_7$–AB) micelles before and after loading PHK at 25 °C. In salt-free solution, the reduced viscosity, η_{sp}/C_p, increases with decreasing C_p, a well-known behavior in salt-free dilute polyelectrolyte solution. At [PHK]/[P(ST–C$_7$–AB)] = 0.5, the value of η_{sp}/C_p decreases compared to the former, because of the decrease of electrostatic interaction. In contrast, in dilute solution of C_p < 0.5 g/dL and [PHK]/[P(ST–C$_7$–AB)] = 1.0, the value of η_{sp}/C_p is low, but the viscosity steeply increases with C_p at values higher than 0.7 g/dL. At C_p > 1.0 g/dL, pronounced viscoelasticity is observed. This may be attributed to the fact that P(ST–C$_7$–AB)-PH$^-$ complex further intermolecularly associates to afford a network structure. It can be concluded from ^{1}H NMR spectroscopy as mentioned above that the intermolecular association of the micelle caused by PHK molecules is reasonably interpreted by intermolecular hydrogen bonding between the carboxyl acid groups of the PH$^-$ ion strongly bound to the ammonium head group of the polymer micelle. The rheological behavior of the systems is now under study and will be reported soon.

Conclusions

The solubilization of aromatic compounds into monomer (ST–C$_7$–AB) micelles and P(ST–C$_m$–AB) micelles has been investigated by ^{1}H NMR spectroscopy. Amphiphilic P(ST–C$_m$–AB) sufficiently solubilizes some hydrophobic aromatic molecules such as methyl benzoate and also acts as an efficient host to strongly capture the hydrophobic counteranions B$^-$, PH$^-$, and Sal$^-$ but not MA$^-$ and FA$^-$. ^{1}H NMR signals of the hydrophobic counteranions are shifted and broadened in water by the presence of the amphiphilic polyelectrolytes. The capturing of hydrophobic counterions by the polyelectrolytes is likely due to electrostatic, hydrophobic, and cation–π interactions between them. PH$^-$ and Sal$^-$ counteranions strongly captured in the vicinity of a polyelectrolyte chain further promote intermolecular association through intermolecular hydrogen bonding between the acid groups. The observed specific interactions may be expected to extend to the design of some supermolecular architectures from proper combination of amphiphilic polyelectrolytes and aromatic acid salts.

Acknowledgements This work was supported in part by a Grant-in-Aid (No. 09875236) and (No. 13650943) from the Ministry of Education, Science, Culture and Sports, Japan.

References

1. Laughlin RG (1994) The aqueous behavior of surfactants. Academic, San Diego
2. Glass JE (ed) (1989) Polymers in aqueous media: performance through association. American Chemical Society, Washington, p 223
3. Shalaby SW, McCormick CL, Butler GB (eds) (1991) Water-soluble polymers: synthesis, solution properties, and applications. American Chemical Society, Washington, vol 467
4. Morishima Y (1994) Trends Polym Sci 2:31
5. Lindman B, Thalberg K (1993) In: Goddard ED, Ananthapadmanabhan KP (eds) Interactions of surfactants with polymers and proteins. CRC, Boca Raton, p 203
6. Paleos CM (1992) In: Paleos CM (ed) Polymerization in organized media. Gordon and Breach, Philadelphia, p 183
7. Larrabee CE, Sprague ED (1979) J Polym Sci B 17:749
8. McGrath KM, Drummond CJ (1996) Colloid Polym Sci 274:316
9. Thundathil R, Stoffer JO, Friberg SE (1980) J Polym Sci A1 18:2629
10. Kline SR (1999) Langmuir 15:2726
11. Shikata T, Hirata H, Kotaka T (1987) Langmuir 3:1081
12. Nakamura K, Yamagata K, Shikata T (2003) Langmuir 19:8654
13. Nakamura K, Shikata T (2003) Macromolecules 36:9698
14. Wu H, Kawaguchi S, Ito K (2004) Colloid Polymer Sci (in press)
15. Kawaguchi S, Imai G, Suzuki J, Miyahara A, Kitano T, Ito K (1997) Polymer 38:2885
16. Eriksson JC, Gillberg G II (1966) Acta Chem Scan 20:2019
17. Lindblom G, Lindman B, Mandell L (1973) J Colloid Interface Sci 42:400
18. Bunton CA, Cowell CP (1988) J Colloid Interface Sci 122:154
19. Ganesh KN, Mitra P, Balasubramanian D (1982) J Phys Chem 86:4291
20. Tokiwa F, Tsujii K (1971) J Phys Chem 75:3560
21. Fendler EJ, Day CL, Fendler JH (1972) J Phys Chem 70:1460
22. Fornasiero D, Grieser F, Sawyer WH (1988) J Phys Chem 92:2301
23. Thomas JK, Grieser F, Wong M (1978) Ber Bunsen Phys Chem 82:937
24. Almgren M, Grieser F, Thomas JK (1989) J Am Chem Soc 707:279
25. Hirose C, Sepulveda L (1981) J Phys Chem 85:3689
26. Rehfeld SJ (1971) J Phys Chem 75:3905
27. Simon SA, McDaniel RV, Mclntosh TJ (1982) J Phys Chem 86:1449
28. Eriksson JC, Gillberg G (1966) Acta Chem Scand 20:2019
29. Fendler JH, Patterson LK (1971) J Phys Chem 75:3907
30. Nagarajan R, Chaiko MA, Ruckenstein E (1984) J Phys Chem 88:2916
31. Kawaguchi S, Toui S, Onodera M, Ito K, Minakata A (1993) Macromolecules 26:3081
32. Manning GS (1969) J Chem Phys 51:924
33. Roelens S, Torriti R (1999) Supramol Chem 10:225
34. Daniels R, Kormendy CG (1962) J Org Chem 27:1860
35. Connors KA (1987) Binding constants. Wiley, New York
36. Wang T, Bradshaw JS, Izatt RM (1994) J Heterocyclic Chem 31:1097
37. Wong KF, Ng S (1976) Spectrochim Acta 32A:455